Journal of Applied Physics

Field-cooled magnetization of Y-Ba-Cu-O superconducting bulk pair reinforced by full metal encapsulation under high magnetic fields up to 22 T

Cite as: J. Appl. Phys. **126**, 243901 (2019); https://doi.org/10.1063/1.5124010
Submitted: 09 August 2019 . Accepted: 07 December 2019 . Published Online: 23 December 2019

Tomoyuki Naito, Hiroyuki Fujishiro, and Satoshi Awaji

AIP Publishing

Field-cooled magnetization of Y-Ba-Cu-O superconducting bulk pair reinforced by full metal encapsulation under high magnetic fields up to 22 T

Cite as: J. Appl. Phys. **126**, 243901 (2019); doi: 10.1063/1.5124010
Submitted: 9 August 2019 · Accepted: 7 December 2019 ·
Published Online: 23 December 2019

View Online Export Citation CrossMark

Tomoyuki Naito,[1,a)] Hiroyuki Fujishiro,[1] and Satoshi Awaji[2]

AFFILIATIONS

[1]Faculty of Science and Engineering, Iwate University, Morioka 020-8551, Japan
[2]High Field Laboratory for Superconducting Materials, Institute for Materials Research, Tohoku University, Sendai 980-8577, Japan

[a)]**Electronic mail:** tnaito@iwate-u.ac.jp

ABSTRACT

We report on the field-cooled magnetization (FCM) process under magnetic fields of up to 22 T for the stacked Y-Ba-Cu-O (YBCO) bulk pair reinforced by a stainless steel (SUS316) container. On the basis of the numerically simulated mechanical stress in a bulk during FCM, the SUS316 container was designed by the numerical simulation to offer the sufficient hoop stress tolerance to the bulk trapping the magnetic field of 20 T. As a result, we obtained successfully the trapped field, B^{T}, of 15.1 T by FCM from 18 T at 28 K at the center of the YBCO bulk pair. However, the extremely large-scale vortex jumps and large temperature rise occurred suddenly during FCM from a higher field of 22 T at a lower temperature of 23 K, and then a small crack was confirmed at the periphery of "both" YBCO bulks from the distorted contour maps of B^{T}. The simultaneous break of both YBCO bulks probably in spite of sufficient mechanical reinforcement led us to conclude that the thermal instability triggered off the large-scale vortex jumps and large heat generation. The stress concentration induced thermally at the hot spot brought about the cracking.

I. INTRODUCTION

Two kinds of superconducting magnets, a conventional coil magnet and a quasipermanent bulk magnet, are well known. Although not only the shape and structure but also the excitation method is completely different from each other, both magnets interestingly have the same crucial issues relating to the electromagnetic stress tolerance under a strong magnetic field generalized by themselves.

The superconducting wires in a coil magnet experience both compressive and tensile stresses on cooling and under the excitation, which deteriorates the superconducting properties such as the upper critical field, B_{c2}, and the critical current density, J_c.[1–4] Specifically, the tensile hoop stress of several hundreds of megapascals by the electromagnetic force along the circumferential direction is applied to the superconductors in a high-field magnet.[5,6] Therefore, to utilize the intrinsic J_c of superconductors and to protect the magnet itself, the superconductors and magnets must be reinforced to withstand the hoop stress. A Ni-based alloy with a high yield stress of 0.8–1.4 GPa at low temperatures[7,8] is well known to be used as a substrate for the $\mathrm{REBa_2Cu_3O_{7-\delta}}$ (RE is the rare earth element, RE123) coated conductors[9] and as a reinforcing lamination for the $\mathrm{(Bi, Pb)_2Sr_2Ca_2Cu_3O_{10+x}}$ wires sheathed with silver alloy.[10] Actually, these wires equipped in the cryogen-free 25 T superconducting magnet at the High Field Laboratory for Superconducting Materials (HFL-SM), Institute for Materials Research (IMR), Tohoku University, have operated safely to date.[5,11,12] In addition to the enhancement of the yield stress of wires, the "Yoroi-coil" was proposed to give structurally an additional stress tolerance to the coil.[13] The double-pancake coils wound with the (Gd,Y)123 coated conductor tapes were fully covered by the glass fiber reinforced plastic (GFRP). As a result, the Yoroi-coil withstood the hoop stress of 2.0 GPa exceeding the yield stress of the Hastelloy substrate (1.3–1.4 GPa), suggesting that the GFRP full-cover successfully took charge of a part of the hoop stress.

Single grain RE-Ba-Cu-O (REBCO) bulks, which mainly consist of the superconducting $\mathrm{REBa_2Cu_3O_{7-\delta}}$ (RE123) matrix and the nonsuperconducting $\mathrm{RE_2BaCuO_5}$ (RE211) phases, are usually reinforced by a metal ring [typically, stainless steel (SUS)] to trap magnetic fields of several Teslas without mechanical fracture.[14] This is because they are the brittle ceramics with quite a low mechanical strength against the electromagnetic tensile hoop stress. The widely scattered fracture strength of 20–160 MPa, which was commonly evaluated by the three point bending test, has been reported for REBCO bulks.[15] This results from the fact that the mechanical strength is sensitive to the microstructure of each tested bulk that contains intrinsically the different amount of voids, impurity particles, crystal defects, and so on. Thus, the enhancement of the internal mechanical strength of bulk is essential. The addition of Ag enhanced the bending strength from 90 MPa of the pristine YBCO bulk to 110–140 MPa of the 10–20 wt. % Ag added one by reducing the preexisting microcracks and preventing the crack propagation.[16] Since the tensile strength is commonly about half of the bending one,[17] we can consider roughly the tensile strength of 50–70 MPa for the Ag-added YBCO bulk. The bending strength of YBCO bulks increased from 76.7 MPa to 115.1 MPa at 77 K by filling up the pores and microcracks in the bulk by the impregnation of epoxy resin.[18] Further external reinforcement by the epoxy resin with carbon fiber realized the trapped field, B^{T}, of 17.24 T at 29 K in the center of the stacked two YBCO bulks by the field-cooled magnetization (FCM) from the applied field, B_{app}, of 18 T.[19] Later, the shrink-fit stainless steel ring, which is a simple and easy reinforcement technique, also enabled to trap a magnetic field of 17.6 T at 26 K in the stacked GdBCO bulk pair, in which B_{app} was also 18 T.[20] The evolution of the shape of the B^{T} profile with respect to temperature, found in both reports, demonstrated that B^{T} of 17 T-class was limited by B_{app} of 18 T and the potential of the REBCO bulks trapping a magnetic field of over 20 T.

The hoop stress tolerance of the cylindrical bulk has often been discussed against the maximum hoop stress, which is proportional to the square of the maximum trapped field, expected at the center of bulk.[21] In a realistic case, on the other hand, the interaction between the bulk and the reinforcing material must be considered. Therefore, we performed the numerical simulations to estimate precisely the hoop stress in the disk bulk during FCM from $B_{\mathrm{app}} = 22$ T to achieve the trapped field of 20 T for two types of reinforcements, a stainless steel (SUS316) ring and a SUS316 full-cover capsule, under three J_c values such as $4J_c^*$, $3J_c^*$, and $2J_c^*$.[22] J_c^* was defined as the critical current density, which was assumed to be independent of the magnetic field, to achieve the trapped field of B^* from the following relation, $B^* = \mu_0 J_c^* R$, by the Bean's critical state model.[23] Here, we used J_c^* of 1.75×10^9 A m^{-2} for B^* of 22 T, μ_0 is the magnetic permeability in vacuum, and R is the radius of disk bulk. For the most severe case of $J_c = 4J_c^*$, we clarified that the bulk encapsulated fully by the SUS316 container withstood the electromagnetic "tensile" hoop stress up to +150 MPa by applying the thermal "compressive" hoop stress of about −200 to −140 MPa, i.e., the net tensile stress was suppressed from +150 MPa to below +10 MPa, rather smaller than the typical tensile strength of +50 to +70 MPa mentioned above.

In this paper, we report the field-cooled magnetization process of the stacked YBCO bulk pair reinforced by the stainless steel capsules, which were expected to apply the sufficient hoop stress tolerance against the trapped field of 20 T by the numerical simulation results,[22] under magnetic fields of up to 22 T at various temperatures of 23–40 K.

II. EXPERIMENTAL PROCEDURE

We stacked two YBCO disk bulks (Bulk#1 and #2) with 20 mm in diameter and 10 mm in thickness reinforced by the stainless steel (SUS316) capsule that consisted of a ring and two thin plates, as shown schematically in Fig. 1. Three-dimensional orthogonal coordinate axes were defined. The x- and y-axes were parallel to the surface of disk bulks and the z-axis along the thickness direction of the bulks, and the origin was set at the center of the stack.

The YBCO bulks were grown by a top seeded melt-growth method at the Nippon Steel Corp.[24] The SUS316 capsules were designed to keep the mechanical strength of bulks against the hoop stress during FCM from the applied magnetic field, B_{app}, of 22 T, which was based on the numerical simulations described elsewhere.[22] Each YBCO bulk was inserted into the SUS316 ring (31 mm in outer diameter, 20 mm in inner diameter, and 10 mm in height), and then covered from both sides by two types of SUS316 thin disk plates, "A" and "B," using six screws. Both plates (A and B) were 31 mm in diameter and 1.5 mm in thickness, and one face of the plate A had a single groove with 3 mm in width and 0.5 mm in depth. As found in Fig. 1, the groove of each plate A, which was faced in stacking the encapsulated YBCO bulks, offered the space with 3 mm in width and 1 mm in height, in which four cryogenic miniature Hall probes (HGT-2010, Lakeshore Inc.) were set at $x = 0$, 2, 5, and 9 mm along the x-axis. It is noteworthy that the seed crystal side and the opposite (bottom) side of each bulk were covered by the plates A and B, respectively, that is, the seed crystal side of each bulk faced each other in the stack. This is because the crystallinity and the superconducting properties are well known to be different from the seed crystal and bottom sides. The temperature of the stacked YBCO bulks was monitored by a Cernox thermometer set at the bottom of the stack.

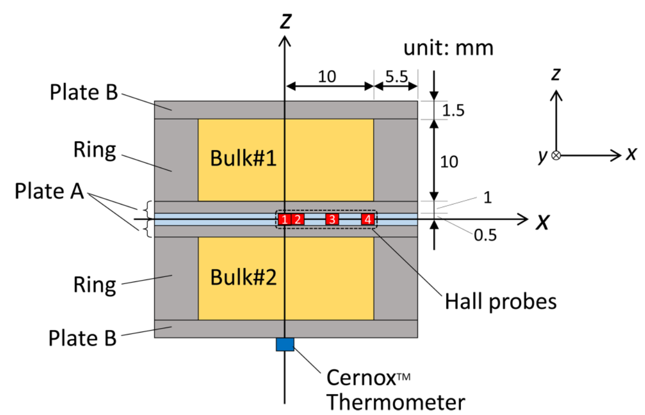

FIG. 1. Schematic image of the stacked YBCO bulk pair (Bulk#1 and #2) reinforced by the stainless steel (SUS316) capsule, which consists of one ring and two different plates A and B. The numbered four small square boxes set along the x-axis are the miniature cryogenic Hall probes. The small square box set at the bottom of the stack is a Cernox thermometer.

The stacked YBCO bulk pair was inserted into a magnetizing coil with a gas He flow type cryostat. The temperature was controlled by the Cernox thermometer and 50 W heater. We used the following two magnets of the HFL-SM, IMR, Tohoku University; one was a commercial cryogen-free 15 T superconducting magnet (JASTEC Inc.), named 15T-CSM, and the other was the specially designed 28 T hybrid magnet consisting of 16 T water-cooled and 12 T superconducting magnets, named 28T-HM. After the FCM experiment under high magnetic fields, the bulk was evaluated by the trapped field profile measured by scanning an axial-type Hall probe (BHA-921, F.W. Bell Inc.) in liquid nitrogen (LN_2) using a commercial cryogen-free 10 T superconducting magnet (JASTEC Inc.) at Iwate University.

III. RESULTS AND DISCUSSION

We measured the local vortex density at four positions, $B_1(x = 0\,\text{mm})$, $B_2(x = 2\,\text{mm})$, $B_3(x = 5\,\text{mm})$, and $B_4(x = 9\,\text{mm})$, and temperature of the stacked YBCO bulk pair during FCM from the initial applied magnetic field, B_{app}, of 15 T at two temperatures of sample, T_s's, 40 and 30 K using the 15T-CSM magnet.

Figure 2(a) shows the typical results taken at $T_s = 40$ K as a function of the time step (TS) of the descent of the magnetic field during FCM. TS was defined by the following relation:

$$TS = \frac{B_{app} - B_{ex}}{B_{app}} \times 10, \tag{1}$$

where B_{ex} was the actual external magnetic field, changing from B_{app} ($TS = 0$) down to 0 T ($TS = 10$). B_{ex} was decreased from 15 T down to 0 T at a constant rate of -0.04 T/min. Both local vortex densities, B_1 and B_2, decreased quite moderately and finally reached 10.0 T and 9.35 T, respectively, just at the ramp-end [$B_{ex} = 0$ T ($TS = 10$)] and $T_s = 40$ K, which were the trapped field at $x = 0$ and 2 mm, named B_1^T and B_2^T, respectively. Somewhat quick decrease in B_3 was observed, and the trapped field at $x = 5$ mm, B_3^T, was 6.08 T. B_4 decreased monotonically with B_{ex} and reached 0.59 T at $TS = 10$. One can notice the decay of the trapped fields at $TS = 10$ due to the vortex creep, which will be discussed later (in Fig. 5). The nearly constant temperature was observed during the FCM process, suggesting that the slowly swept B_{ex} suppressed the heat generation due to the vortex dynamics. Note that B_1^T of 13.5 T at the ramp-end was also successfully obtained during FCM from $B_{app} = 15$ T at $T_s = 30$ K (not shown here); the somewhat elevated B_1^T originated from the increase of J_c by lowering T_s.

Figure 2(b) shows the FCM process for the stacked YBCO bulk pair under $B_{app} = 18$ T at $T_s = 28$ K using the 28T-HM magnet. As shown schematically in the inset of Fig. 2(b), B_{ex} was decreased stepwise from 18 T down to 0 T, to avoid the heat generation due to the vortex dynamics by the high sweep rate, -0.20 to -0.32 T/min, of 28T-HM. The interval of the applied magnetic field, ΔB_{ex}, was -0.05 to -0.1 T with the duration, Δt, of 0.5 min, which corresponded to the pseudo-sweep rate of about -0.1 to -0.2 T/min. Although the gradual decrease of the vortex density was observed below $TS = 6$, the vortices began to be excluded swiftly beyond $TS = 6$. Consequently, the YBCO bulk pair trapped successfully the magnetic field of 15.1 T at $x = 0$ mm just at the ramp end. The temperature was stable during FCM, although the present 28T-HM experiment had somewhat faster pseudo-sweep rate of B_{ex} than that in the 15T-CSM experiments. No vortex jumps and no abrupt temperature rise suggest strongly that both YBCO bulks were protected during FCM from 18 T by the present SUS316 capsules, as expected from the numerical simulation results.[22] In addition, we confirmed that this YBCO bulk pair trapped 15.1 T again in the second FCM experiment under the same condition ($B_{app} = 18$ T and $T_s = 28$ K), which also support no fracture of both bulks. If a crack was created at the first FCM experiment, the second trapped field should deteriorate by the crack propagation.

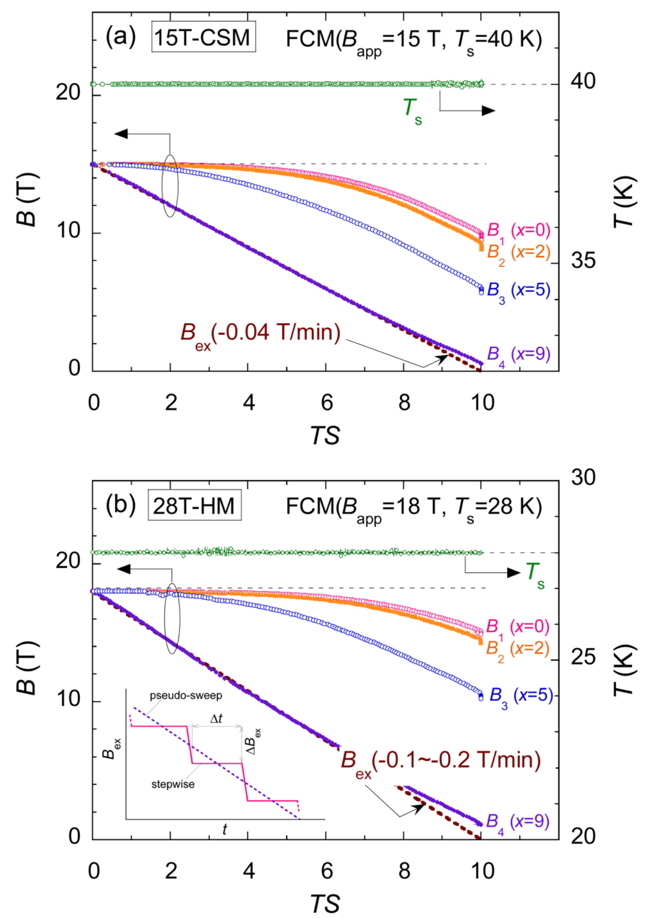

FIG. 2. Time step (TS) dependence of the local vortex density (left vertical axis) and temperature (right vertical axis) of the stacked YBCO bulk pair during the FCM process under (a) $B_{app} = 15$ T and $T_s = 40$ K and (b) $B_{app} = 18$ T and $T_s = 28$ K, respectively. The inset of (b) shows schematically the stepwise change and the pseudoswept B_{ex} as a function of time, t.

Figure 3 shows the mappings of trapped field, B^T, in the x-y plane, which were taken at 2.5 mm distance from both surfaces of YBCO bulks after FCM under $B_{app} = 1$ T in LN_2. The concentric

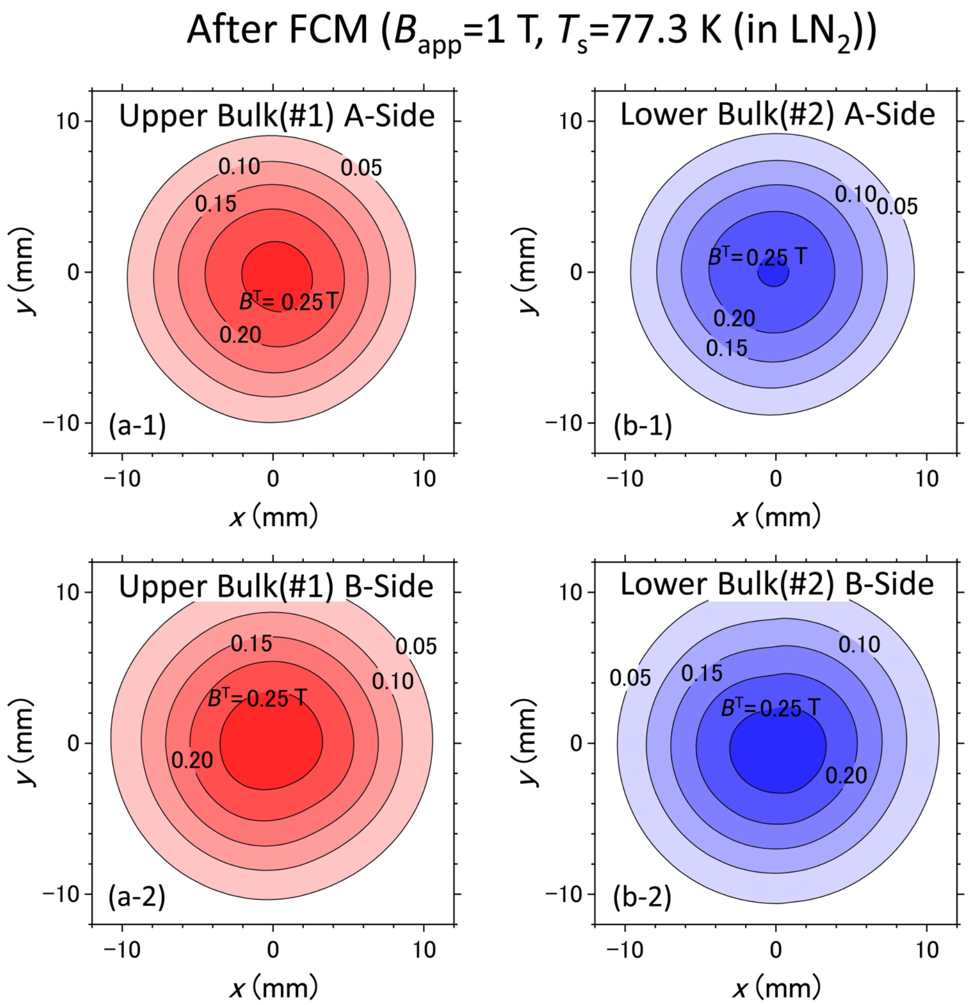

FIG. 3. The profile of the trapped magnetic field at 2.5 mm distance from the surface of bulk for each YBCO bulk after FCM under $B_{app} = 1$ T in the liquid nitrogen. (a-1) and (a-2), respectively, are for the plate A and B sides of the #1 bulk (Upper bulk). (b-1) and (b-2), respectively, are for the plate A and B sides of the #2 bulk (Lower bulk).

circular profiles without the distortion were observed at each surface of both upper #1 and lower #2 bulks. This also supports strongly no fracture of both bulks during FCM under $B_{app} = 18$ T at $T_s = 28$ K. If the cracking happens partially in a bulk during FCM, the induced supercurrent should circumvent a crack, resulting in the distorted B^T profile. The maximum trapped fields, $B^{T,\ max}$'s, were 0.27 and 0.28 T, respectively, at the plates A (seed crystal) and B (bottom) sides for the upper #1 bulk, and those were 0.25 and 0.28 T for the lower #2 bulk. Somewhat higher trapped fields with larger area at the plate B (bottom) side than those at the plate A (seed crystal) one are found for both bulks. This difference seems to originate from the low superconducting properties of the seed crystal side because of the existence of the $a(b)$-growth region with relatively low crystallinity and less Y211 particles acting as the pinning centers.

Figure 4 shows the trapped field profile, $B^T(x)$, just at the ramp-end under various indicated FCM conditions for the stacked YBCO bulk pair. The domelike shaped $B^T(x)$ came from the magnetic field dependent $J_c(B)$, which suggested that the induced supercurrent flew through the whole region of bulks, that is, both YBCO bulks were fully magnetized. B^T independent of x should appear, if a region with no induced supercurrent flowing exists.

Figure 5 shows the time dependence of the reduced trapped field at the center ($x = 0$ mm), $B_1^T(t)/B_1^T(0)$, of the stacked YBCO bulk pair for various FCM conditions. The start time, $t = 0$ min, was defined as the time at the ramp-end. The lower two experimental data were taken using the 15T-CSM. At $T_s = 40$ K, the trapped field began to decay steeply around $t = 5$ min, and the decay of about 3% was observed at $t = 10$ min. The decay became moderate at a lower temperature of $T_s = 30$ K, because the increase of pinning potential and the decrease of thermal fluctuation were brought about simultaneously by lowering temperature. As a result, the 3% decay of B_1^T was observed at $t = 50$ min. However, B_1^T after FCM under $B_{app} = 18$ T at $T_s = 28$ K using the 28T-HM decayed somewhat rapidly just like as at $T_s = 40$ K using the 15T-CSM. This indicates that more vortices were activated in the 28T-HM experiment, compared to the 15T-CSM one with the sweep rate of -0.04 T/min, by the

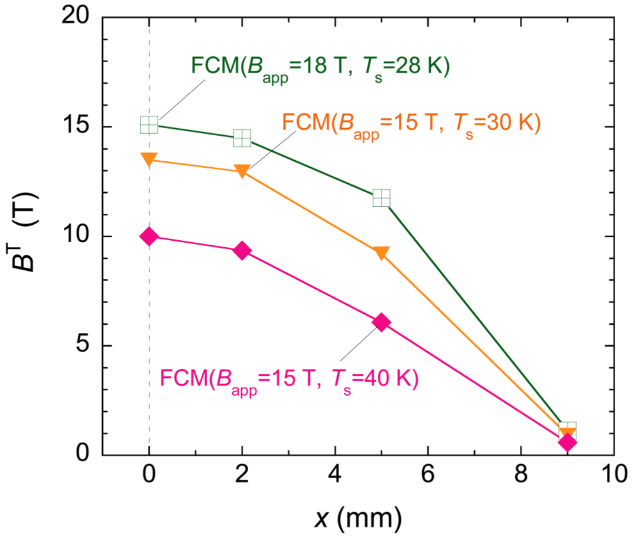

FIG. 4. Trapped field at the ramp-end along the x-axis for the stacked YBCO bulk pair under various indicated FCM conditions.

larger induced electromotive force, $d\Phi/dt(=d(B_{ex}S)/dt)$, at the change in B_{ex}, which depends on the original sweep rate of the 28T-HM (-0.20 to -0.32 T/min). Here, Φ is the magnetic flux, and S is the cross-sectional area of bulk surface perpendicular to the z-axis.

Figure 6 shows the trapped field at $x = 0$ mm, $B_1^T(T)$, as a function of the temperature after the successful FCM experiment at $B_{app} = 18$ T and $T_s = 28$ K for the stacked YBCO bulk pair. $B_1^T(T)$ decreased monotonically with the negative curvature with increasing temperature. No temperature-independent $B_1^T(T)$ also supports that both YBCO bulks were fully magnetized. Extrapolating of this curve toward the low temperatures suggested that the trapped field over 20 T can be achieved below 20 K for this YBCO bulk pair.

To obtain a higher trapped field, therefore, the FCM experiment was performed at the lower temperature of $T_s = 23$ K under $B_{app} = 22$ T for the same YBCO bulk pair using the 28T-HM, as shown in Fig. 7; the target trapped field was not 20 T but 18 T to avert the thermal instability. B_{ex} was decreased from 22 T down to 20 T with somewhat fast constant sweep rate of -0.2 T/min, and subsequently stepwise with $\Delta B_{ex} = -0.05$ T and $\Delta t = 0.5$ min. Both local vortex densities, B_1 and B_2, decreased moderately with

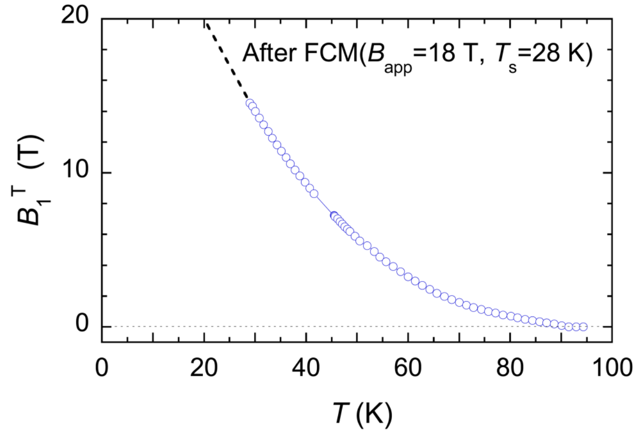

FIG. 6. Temperature dependence of the trapped field at $x = 0$ mm, $B_1^T(T)$ of the stacked YBCO bulk pair after FCM from $B_{app} = 18$ T at 28 K.

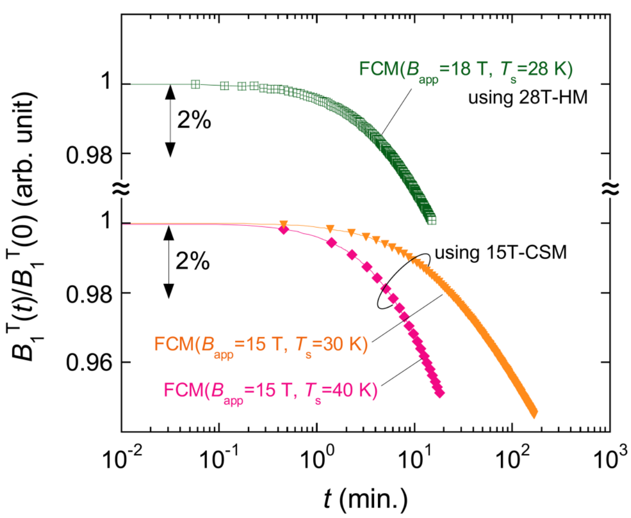

FIG. 5. Time dependence of the reduced trapped field at the center ($x = 0$ mm), B_1^T, of the stacked YBCO bulk pair for various indicated FCM conditions.

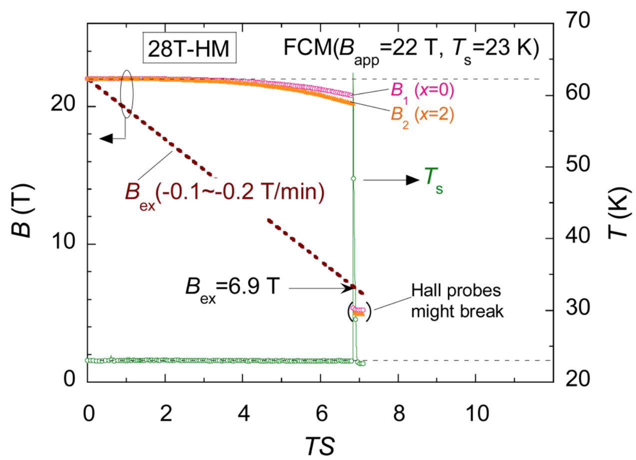

FIG. 7. Time step (TS) dependence of the local vortex density (left vertical axis) and temperature (right vertical axis) of the stacked YBCO bulk pair during the FCM process under $B_{app} = 22$ T and $T_s = 23$ K.

decreasing B_{ex}. However, both B_1 and B_2 jumped abruptly from 20.5 T to (5 T) at $TS = 6.9$ ($B_{ex} = 6.9$ T), and, at the same time, the temperature of the YBCO bulk pair increased steeply from 23 K to ∼ 63 K. Just after the vortex jumps occurred, the B_{ex} sweeping was immediately stopped, and then T_s was increased slowly up to T_c to protect the YBCO bulks from the further crack propagation, assuming that the cracking occurred. Note that both lower B_1 and B_2 compared to B_{ex} at the vortex jumps are artificial because they showed about 5 T even at 100 K. The Hall probes themselves seemed to be broken by the overvoltage due to the large induced electromotive force at the sudden change in the magnetic field.

Figure 8 shows the mappings of the trapped magnetic field at 2.5 mm distance from both surfaces of each YBCO bulk after FCM under $B_{app} = 1$ T in LN_2. The degradation of $B^{T,\,max}$ from 0.27 T down to 0.25 T and the distorted B^T profile were found at the plate A side of the upper #1 bulk [Fig. 8(a-1)]. On the other hand, $B^{T,\,max}$ was kept as high as 0.28 T at the plate B side of the upper #1 bulk, although the B^T profile was slightly distorted, as shown in Fig. 8(a-2). Further deterioration of $B^{T,\,max}$ and distortion of the B^T profiles were observed for the lower #2 bulk; $B^{T,\,max}$'s of the plate A and B sides, respectively, decreased from 0.25 T down to 0.20 T and from 0.28 T down to 0.24 T. These results indicate that the cracking occurred at the periphery of the plate A side for both YBCO bulks, and the size of crack of lower #2 bulk seems to be larger than that of upper #1 bulk.

The vortex jumps originate possibly from the bulk fracture or thermal instability. First, let us consider the vortex jumps triggered by the partial fracture of YBCO bulks at the periphery in spite of the mechanical reinforcement. In our simulation results for the same experimental setup and condition ($B_{app} = 22$ T), the trapped fields at the center ($x = y = z = 0$ mm), $B^{T(sim)}$'s, of 21.5, 21.1, and 18.8 T, respectively, were estimated for three J_c values such as $4J_c^*$, $3J_c^*$ and $2J_c^*$.[22] Thus, B^T of 18 T expected experimentally suggests that J_c of the present YBCO bulks at 23 K is probably somewhat smaller than $2J_c^*$. For $J_c = 2J_c^*$, the bulk encapsulated by the present SUS316 capsule felt only the compressive stress during FCM from $B_{app} = 22$ T and under $B^T = 18.8$ T.[22] One can notice that an area between the fixing screws might weaken the reinforcement

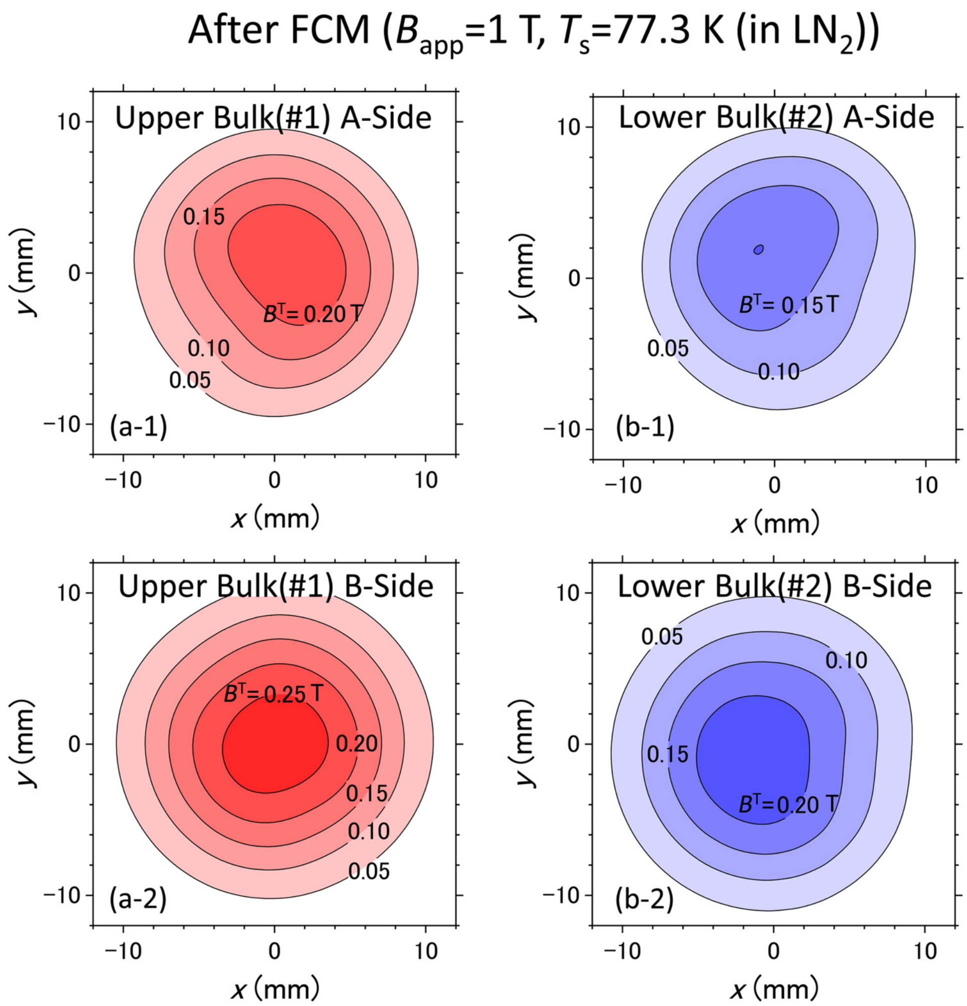

FIG. 8. The profile of trapped magnetic field at 2.5 mm distance from the surface of bulk for each YBCO bulks after the FCM under $B_{app} = 1$ T in the liquid nitrogen. (a-1) and (a-2), respectively, are for the plate A and B sides of the #1 bulk (Upper bulk). (b-1) and (b-2), respectively, are for the plate A and B sides of the #2 bulk (Lower bulk).

mechanically; however, only the SUS316 ring (without flaps) was confirmed numerically to apply the compressive stress of about −100 MPa thermally to the periphery of bulk.[22] In any case, the bulk fracture should not happen at the periphery under the present mechanical reinforcement. In addition, the observed one large vortex jumps during FCM indicates that the present two YBCO bulks probably broke simultaneously. Because of the different microstructure of each bulk, it is extremely difficult to consider that a lack of mechanical reinforcement causes the bulk fracture "simultaneously." Thus, we conclude that the YBCO bulks were protected mechanically by the present SUS316 capsules, as expected, and have to consider an alternative possibility of the bulk fracture.

Next, we consider the influence of thermal shock due to the abrupt local heat generation by the vortex jumps on the mechanical behavior. This is because the vortex jumps are usually known to be caused by the thermal instability owing to the small specific heat of the bulk at low temperatures. The local heat generation leads the temperature gradient in the bulk, which results in the thermal compressive stress at the hot spot under the conditions that restrain free expansion. In addition, the sudden decrease in both B^{T} and J_c reduces quickly the electromagnetic hoop stress, and then the bulk might be subjected to the additional compressive stress by the sudden contraction. There are a few reports for the compressive tests of REBCO bulks.[25,26] The compressive strength of a YBCO bulk was reported to be over 196 and 115 MPa along the *c*-axis and the *ab*-planes, respectively.[25] For a SmBCO bulk, the average compressive strengths were 466 and 368 MPa along the *c*-axis and the *ab*-planes, respectively.[26] The cleavage at the *ab*-planes gives rise to the lower compressive strength along the *ab*-plane. Therefore, the compressive stress of several hundreds of megapascals is required to break the bulk.

The thermal stress at any point, σ^{th}, which depends on the difference in temperature between that point, T_{p}, and the average, T_{ave}, of an infinite slab sample, is given by the following relation:[27]

$$\sigma^{\mathrm{th}} = \frac{E\alpha}{1-\nu}(T_{\mathrm{ave}} - T_{\mathrm{p}}), \tag{2}$$

where E is Young's modulus, α is the liner thermal expansion coefficient, and ν is the Poisson ratio. Using the typical mechanical parameters of REBCO bulks, $E = 100$ GPa, $\alpha = 5.2 \times 10^{-6}\ \mathrm{K}^{-1}$, and $\nu = 0.33$, $\sigma^{\mathrm{th}} = 0.78 \times (T_{\mathrm{ave}} - T_{\mathrm{p}})$ is obtained. This relation suggests that the temperature rise over 200 K is roughly needed to induce the bulk fracture thermally, however, that at the vortex jumps was as low as approximately 40 K, as found in Fig. 7. Considering the position of the Cernox thermometer and the low thermal conductive REBCO bulks,[28,29] the actual temperature rise at the hot spot must be rather larger than the observed experimentally. The thermal shock effect proposed here will be confirmed by the numerical simulations combined with the direct observation of the cracks by the X-ray CT technique[30] in the near future. In addition to the mechanical strength, the thermal stability is also a crucial important issue to realize the trapped field over 20 T, which can be solved by inserting a high thermal conductive metal as the heat sink to the bulk.[18]

IV. CONCLUSION

We have studied the field-cooled magnetization (FCM) of stacked Y-Ba-Cu-O (YBCO) bulk pair reinforced by the stainless steel (SUS316) capsule under magnetic fields of up to 22 T. The SUS316 capsule was designed to apply the sufficient compressive stress to the YBCO bulks overcoming the electromagnetic tensile stress during FCM from 22 T, which was based on the numerical simulations reported previously. As a result, the trapped field, B^{T}, of 15.1 T at 28 K was successfully achieved at the center of YBCO bulk stack. However, the FCM experiment under the magnetic field of 22 T at 23 K failed, that is, the huge vortex jumps occurred during the withdrawal of the external magnetic field. The small crack was confirmed at the periphery by the two-dimensional B^{T} profiles for both YBCO bulks. The break of both YBCO bulks, in spite of the sufficient mechanical strength estimated by the numerical simulation, suggested to originate not from a lack of mechanical reinforcement but from a thermal shock by the heat generation due to the abrupt and remarkably large change in the vortex density in the YBCO bulk stack. The importance of the control of the exhaust heat from the bulk was suggested in addition to the mechanical strength.

ACKNOWLEDGMENTS

The authors would like to thank Mr. Y. Sasaki, Mr. K. Fushimi, and Mr. H. Ishikawa of the High Field Laboratory for Superconducting Materials, Institute for Materials Research, Tohoku University for their assistance in the experiments using a Hybrid magnet, 28T-HM. We also thank Mr. Y. Takeda, Mr. Yuhei Takahashi, and Mr. Yuya Takahashi of the Iwate University for their help in part of this work. This work was partly supported by JSPS KAKENHI under Grant Nos. JP15K04718, JP15K04646, and JP18K04920.

REFERENCES

[1]J. W. Ekin, IEEE Trans. Magn. **17**, 658 (1981).
[2]H. Sakamoto, S. Endoh, Y. Nagasu, K. Wada, A. Kimura, S.-I. Meguro, S. Awaji, K. Watanabe, and M. Motokawa, IEEE Trans. Appl. Supercond. **12**, 1067 (2002).
[3]K. Osamura, S. Machiya, H. Suzuki, S. Ochiai, H. Adachi, N. Ayai, K. Hayashi, and K. Sato, Supercond. Sci. Technol. **21**, 054010 (2008).
[4]M. Sugano, K. Shikimachi, N. Hirano, and S. Nagaya, Supercond. Sci. Technol. **23**, 085013 (2010).
[5]K. Watanabe, S. Awaji, H. Oguro, Y. Tsuchiya, S. Hanai, H. Miyazaki, T. Tosaka, M. Takahashi, and S. Ioka, J. Phys. Conf. Ser. **568**, 032019 (2014).
[6]Y. Yanagisawa, Y. Xu, S. Iguchi, M. Hamada, S. Matsumoto, G. Nishijima, H. Nakagome, T. Takao, H. Suematsu, Y. Oshima, X. Jin, M. Takahashi, and H. Maeda, Supercond. Sci. Technol. **28**, 125005 (2015).
[7]C. Clickner, J. Ekin, N. Cheggour, C. Thieme, Y. Qiao, Y. Xie, and A. Goyal, Cryogenics **46**, 432 (2006).
[8]M. Sugano, K. Osamura, W. Prusseit, H. Adachi, and F. Kametani, IEEE Trans. Appl. Supercond. **17**, 3040 (2007).
[9]Y. Iijima, N. Tanabe, O. Kohno, and Y. Ikeno, Appl. Phys. Lett. **60**, 769 (1992).
[10]T. Nakashima, K. Yamazaki, S. Kobayashi, T. Kagiyama, M. Kikuchi, S. Takeda, G. Osabe, J. Fujikami, and K. Osamura, IEEE Trans. Appl. Supercond. **25**, 1 (2015).
[11]S. Hanai, T. Tsuchihashi, S. Ioka, K. Watanabe, S. Awaji, and H. Oguro, IEEE Trans. Appl. Supercond. **27**, 1 (2017).

[12]S. Awaji, K. Watanabe, H. Oguro, H. Miyazaki, S. Hanai, T. Tosaka, and S. Ioka, Supercond. Sci. Technol. **30**, 065001 (2017).
[13]T. Watanabe, S. Nagaya, N. Hirano, S. Awaji, H. Oguro, Y. Tsuchiya, T. Omura, S. Nimori, T. Shimizu, A. Ishiyama, and X. Wang, IEEE Trans. Appl. Supercond. **25**, 1 (2015).
[14]H. Teshima, M. Morita, T. Arayashiki, T. Naito, and H. Fujishiro, Phys. Procedia **45**, 61 (2013).
[15]K. Katagiri, A. Murakami, and K. Kasaba, Cryogenics **48**, 87 (2008).
[16]H. Fujimoto, Supercond. Sci. Technol. **16**, 1115 (2003).
[17]K. Katagiri, A. Murakami, Y. Shoji, H. Teshima, M. Sawamura, A. Iwamoto, T. Mito, and M. Murakami, Physica C **412–414**, 633 (2004).
[18]M. Tomita, M. Murakami, and K. Katagiri, Physica C **378–381**, 783 (2002).
[19]M. Tomita and M. Murakami, Nature **421**, 517 (2003).
[20]J. H. Durrell, A. R. Dennis, J. Jaroszynski, M. D. Ainslie, K. G. B. Palmer, Y.-H. Shi, A. M. Campbell, J. Hull, M. Strasik, E. E. Hellstrom, and D. A. Cardwell, Supercond. Sci. Technol. **27**, 082001 (2014).
[21]E. Collings and M. D. Sumption, in *Proceedings of the Fourth International Conference and Exhibition: World Congress on Superconductivity*, edited by K. Krishen and C. Burnham (NASA Conference Publication, 1994), Vol. I, pp. 138–147.
[22]H. Fujishiro, T. Naito, and S. Awaji, Supercond. Sci. Technol. **32**, 045005 (2019).
[23]C. P. Bean, Phys. Rev. Lett. **8**, 250 (1962).
[24]M. Morita, M. Sawamura, S. Takebayashi, K. Kimura, H. Teshima, M. Tanaka, K. Miyamoto, and M. Hashimoto, Physica C **235–240**, 209 (1994).
[25]N. Sakai, F. Munakata, P. Diko, S. Takebayashi, S.-I. Yoo, and M. Murakami, in *Advances in Superconductivity X*, edited by K. Osamura and I. Hirabayashi (Springer, 1998), pp. 645–648.
[26]A. Murakami, K. Katagiri, R. Kan, H. Miyata, Y. Shoji, K. Noto, A. Iwamoto, and T. Mito, Physica C **426–431**, 644 (2005).
[27]W. Kingery, H. Bowen, and D. Uhlmann, *Introduction to Ceramics* (Wiley-Interscience Publication, 1976).
[28]H. Fujishiro, M. Ikebe, T. Naito, K. Noto, S. Kohayashi, and S. Yoshizawa, Jpn. J. Appl. Phys. **33**, 4965 (1994).
[29]H. Fujishiro, K. Katagiri, A. Murakami, Y. Yoshino, and K. Noto, Physica C **426–431**, 699 (2005).
[30]M. Inoue, H. Tatara, K. Harada, K. Higashikawa, S. Ye, A. Matsumoto, H. Kumakura, and T. Kiss, IEEE Trans. Appl. Supercond. **26**, 6201004 (2016).